
Graph Optimal Transport with Transition Couplings of Random Walks

Kevin O'Connor
UNC Chapel Hill
koconn@live.unc.edu

Bongsoo Yi
UNC Chapel Hill
bongsoo@unc.edu

Kevin McGoff
UNC Charlotte
kmcgoff1@uncc.edu

Andrew B. Nobel
UNC Chapel Hill
nobel@email.unc.edu

Abstract

We present a novel approach to optimal transport between graphs from the perspective of stationary Markov chains. A weighted graph may be associated with a stationary Markov chain by means of a random walk on the vertex set with transition distributions depending on the edge weights of the graph. After drawing this connection, we describe how optimal transport techniques for stationary Markov chains may be used in order to perform comparison and alignment of the graphs under study. In particular, we propose the graph optimal transition coupling problem, referred to as GraphOTC, in which the Markov chains associated to two given graphs are optimally synchronized to minimize an expected cost. The joint synchronized chain yields an alignment of the vertices and edges in the two graphs, and the expected cost of the synchronized chain acts as a measure of distance or dissimilarity between the two graphs. We demonstrate that GraphOTC performs equal to or better than existing state-of-the-art techniques in graph optimal transport for several tasks and datasets. Finally, we also describe a generalization of the GraphOTC problem, called the FusedOTC problem, from which we recover the GraphOTC and OT costs as special cases.

1 Introduction

In graph comparison tasks, one aims to assess the similarity or dissimilarity of two graphs by means of their topologies and vertex characteristics. In graph alignment or matching tasks, one aims to associate the vertices and edges in a graph with similar vertices and edges in another graph. Both comparison and alignment are of fundamental importance in the study of graphs in machine learning and data science. Examples of applications include image captioning [8], object recognition [38], domain adaptation [22], aligning single-cell multi-omics data [11], and language comparison [4].

Some recent work [29, 32, 23, 24, 12] addresses the problems of graph comparison and alignment using techniques from optimal transport. In the optimal transport (OT) problem, one seeks a plan for transporting mass between two probability measures of interest that minimizes expected cost. When each graph under study is associated with a probability distribution and a cost or distance between the vertices in each pair of graphs is available, graph comparison and alignment both fit naturally into the framework of OT. In particular, optimal transport plans between the probability distributions correspond to alignments between the graphs, while the expected cost of transportation serves as a measure of dissimilarity or distance between graphs of interest.

To date, most OT-based approaches to graph comparison and alignment fall into one of two categories: spectral methods or methods based on the Gromov-Wasserstein distance. In the spectral approaches,

each graph is associated with a zero-mean, multivariate normal distribution whose covariance matrix is a function of the graph Laplacian. Graph OT is then performed via OT between the associated normal distributions of the graphs of interest. In theory and example, one finds that these methods emphasize differences in global structure, i.e., graph structure that is robust to small changes in vertices and edges. On the other hand, the Gromov-Wasserstein approach associates each graph with a discrete distribution over its vertex set and aims to couple these probability measures so as to minimize changes in the edge weights of either graph. The resulting graph OT problem emphasizes differences in local structure over global structure.

In this paper, we describe a novel approach to OT for graph comparison and alignment that balances differences in both global and local structure. We first propose to associate each graph with a stationary Markov chain on its vertex set, with transition probabilities depending on the edge weights of the graph. After drawing this connection, we define an OT problem for graphs by means of an OT problem between the associated Markov chains of the graphs of interest. Leveraging recent work in OT for Markov chains, we define the GraphOTC problem, which aims to find a product graph with an associated Markov chain that minimizes the expectation of the pre-specified cost with respect to the chain’s stationary distribution. This new approach can incorporate local structure by means of the cost function between the vertices of either graph, and it accounts for global structure via the stationary distributions of the associated Markov chains. GraphOTC can easily accommodate many distinct types of cost functions, including cost functions that depend on the intrinsic local structure of the graphs and cost functions that involve external features of the nodes. Furthermore, GraphOTC is easily interpretable and does not rely on selecting any free parameters. Finally, drawing inspiration from the Fused Gromov-Wasserstein problem [32], we situate the GraphOTC problem within a broader theoretical context via a graph OT framework that we call FusedOTC.

Contributions. The contributions of this paper are as follows: (a) we define the GraphOTC problem for graphs that extends OT techniques for Markov chains to graphs; (b) we demonstrate that when the underlying cost satisfies the properties of a metric, the associated GraphOTC cost is a metric on certain equivalence classes of graphs; (c) we demonstrate that the performance of GraphOTC equals or surpasses the state-of-the-art in graph OT for several graph alignment and graph comparison tasks; (d) we describe a broader graph OT framework, known as FusedOTC, that includes the GraphOTC and OT costs as special cases.

1.1 Related work

Spectral methods. One line of work [23, 24, 12] uses graph spectral techniques to define OT problems for graphs. In particular, this approach associates to each graph a multivariate Gaussian with zero mean and covariance matrix equal to the pseudoinverse of the graph Laplacian. The Wasserstein distance between Gaussians in the same space may be computed analytically in terms of the respective covariance matrices. For graphs with different numbers of vertices, [24] and [12] propose to optimize this distance over soft many-to-one assignments between vertices in either graph. At present, this family of approaches is unable to incorporate available feature information or underlying cost functions, relying completely on intrinsic structure in their respective optimization problems.

Variants of Gromov-Wasserstein. Another line of work [25, 29, 32, 34, 33] considers the Gromov-Wasserstein (GW) distance and related extensions. In this work, one tries to couple distributions on the nodes in each graph so as to minimize an expected transport cost between vertices while minimizing changes in edges between the two graphs. This approach allows one to capture differences in both features and structure between graphs. We refer the reader to [12] for a discussion on the differences between spectral-based graph OT methods and GW distances. A number of variants of the GW distance have been proposed for a variety of tasks including cross-domain alignment [8], graph partitioning [35], graph matching [35, 36], and node embedding [36]. The work [5] proposes to incorporate global structure into the Wasserstein and Fused GW distances by applying a heat diffusion to the vertex features before computing the cost matrix.

2 Preliminaries

Notation. Let \mathbb{R}_+ be the set of non-negative real numbers and for every $n \geq 1$, let $\Delta_n = \{\mu \in \mathbb{R}_+^n \mid \sum_{i=1}^n \mu_i = 1\}$ be the probability simplex in \mathbb{R}^n . For a Polish space \mathcal{U} , we will use $\mathcal{M}(\mathcal{U})$ to denote the set of Borel probability measures on \mathcal{U} . Note that whenever the set \mathcal{U} is finite, we will frequently regard probability measures in $\mathcal{M}(\mathcal{U})$ as vectors in $\Delta_{|\mathcal{U}|}$. We define the inner product $\langle \cdot, \cdot \rangle$ for matrices $U, V \in \mathbb{R}^{m \times n}$ by $\langle U, V \rangle = \sum_{i,j} U_{ij} V_{ij}$. For a vector $u \in \mathbb{R}^m$ and matrix $U \in \mathbb{R}^{m \times n}$, we will denote by $u \odot U$ the matrix satisfying $(u \odot U)_{ij} = u_i U_{ij}$. Graphs will be denoted by triples $\mathcal{G} = (V, E, w)$ where V is the vertex set, $E \subset V \times V$ is the edge set, and $w : E \rightarrow \mathbb{R}$ is a function that gives the weight of each edge. All graphs considered in this paper will be assumed to be undirected and connected. For unweighted graphs, we define $w(e) = 0$ for all $e \in E$ by convention.

2.1 Optimal transport

Let $\mu \in \mathcal{M}(\mathcal{U})$ and $\nu \in \mathcal{M}(\mathcal{V})$ be probability measures on finite spaces \mathcal{U} and \mathcal{V} , respectively, and let $c : \mathcal{U} \times \mathcal{V} \rightarrow \mathbb{R}_+$ be a non-negative function. Transport plans in the optimal transport (OT) problem are formalized mathematically as *couplings*: A probability measure $\pi \in \mathcal{M}(\mathcal{U} \times \mathcal{V})$ is a coupling of μ and ν if $\pi \mathbb{1} = \mu$ and $\pi^\top \mathbb{1} = \nu$. We will denote the set of couplings of μ and ν by $\Pi(\mu, \nu)$. The OT problem is to minimize the expectation of c over the set $\Pi(\mu, \nu)$:

$$\min \{ \langle \pi, c \rangle : \pi \in \Pi(\mu, \nu) \}. \quad (1)$$

The optimal value of Problem (1) is referred to as the optimal transport cost and optimal solutions are referred to as optimal transport plans or optimal couplings. For more details on the OT problem in general, the reader may consult [28].

2.2 Optimal transition couplings of Markov chains

In recent work [26], the OT problem (1) has been adapted to the setting of Markov chains, resulting in an optimization problem called the optimal transition coupling (OTC) problem. Let $P \in [0, 1]^{|\mathcal{U}| \times |\mathcal{U}|}$ and $Q \in [0, 1]^{|\mathcal{V}| \times |\mathcal{V}|}$ be aperiodic and irreducible transition matrices on \mathcal{U} and \mathcal{V} , respectively. A transition coupling of P and Q is a transition matrix $R \in [0, 1]^{|\mathcal{U}| \times |\mathcal{V}| \times |\mathcal{U}| \times |\mathcal{V}|}$ satisfying

$$\sum_{\tilde{v} \in \mathcal{V}} R((u, v), (u', \tilde{v})) = P(u, u') \quad \text{and} \quad \sum_{\tilde{u} \in \mathcal{U}} R((u, v), (\tilde{u}, v')) = Q(v, v'),$$

for every $(u, v), (u', v') \in \mathcal{U} \times \mathcal{V}$. In other words, the rows of the joint transition matrix R are couplings of the rows of the transition matrices P and Q . Every transition coupling corresponds to a stationary Markov chain taking values in $\mathcal{U} \times \mathcal{V}$. Furthermore, every such Markov chain is necessarily a coupling of the Markov chains corresponding to the transition matrices P and Q , and thus one may define an OT problem for Markov chains in terms of transition couplings [26]. We will denote the set of transition couplings of P and Q by $\Pi_{\text{TC}}(P, Q)$.

The OTC problem is to minimize the expectation of c over the set of stationary distributions of transition couplings of P and Q :

$$\min \{ \langle \lambda, c \rangle : R \in \Pi_{\text{TC}}(P, Q), \lambda R = \lambda, \lambda \in \Delta_{|\mathcal{U}| \times |\mathcal{V}|} \}. \quad (2)$$

As discussed in [26], one may view the OTC problem as trying to synchronize the Markov chains corresponding to P and Q with respect to the long-run average of the cost c . The optimal pair (λ, R) characterizes the synchronized chain, while the minimal expected cost $\langle \lambda, c \rangle$ provides a measure of dissimilarity between P and Q . Importantly, this dissimilarity measure emphasizes long-term average differences over short-term behavior. This feature is due to the stationarity constraint in the OTC problem and will be key in enabling our proposed approach to graph OT to capture differences in global structure despite being defined in terms of a cost between vertices.

3 GraphOTC

Relationships between graphs and Markov chains have been studied extensively in the literature [21, 3, 20]. We propose to leverage this connection in order to define a new OT problem for graphs.

In particular, we view each graph in terms of a stationary random walk on its vertex set and apply the OT problem to the random walks associated with the graphs of interest. Formally, to any graph $\mathcal{G} = (V, E, w)$, we associate a transition matrix $P \in [0, 1]^{|V| \times |V|}$, defined as follows: Let

$$P(u, u') = \frac{\exp\{w(u, u')\}}{\sum_{\tilde{u}: (u, \tilde{u}) \in E} \exp\{w(u, \tilde{u})\}}, \quad \forall (u, u') \in E,$$

and $P(u, u') = 0$ otherwise. If P is irreducible, then it defines a unique stationary Markov chain, which we also refer to as P when no confusion may arise. Using this construction, connected graphs will correspond to irreducible Markov chains. Moreover, connected graphs with at least one self loop will correspond to aperiodic Markov chains, and we note that any irreducible Markov chain can be made aperiodic by considering the “lazy” chain instead (see [20, p. 9]). For the rest of the paper, we will associate the graphs of interest, \mathcal{G}_1 and \mathcal{G}_2 , with the stationary Markov chains P and Q , respectively. We will also assume for convenience that P and Q are aperiodic and irreducible.

The random walk on a graph encodes important geometric properties of the graph, and it has tight connections to both local properties of the graph (such as edge weights and generalized node degrees) and global properties of the graph (such as the Laplacian and its spectrum). Indeed, the stationary distribution of the random walk gives a notion of the global importance of the vertices within the graph. For these reasons, coupling the random walks of two graphs provides a natural and informative setting for performing graph OT.

In light of this perspective, we now define the GraphOTC problem as

$$d(\mathcal{G}_1, \mathcal{G}_2) = \min \{ \langle \lambda, c \rangle : R \in \Pi_{\text{TC}}(P, Q), \lambda R = \lambda, \lambda \in \Delta_{|V_1| \times |V_2|} \}. \quad (3)$$

Note that in addition to a coupling cost of \mathcal{G}_1 and \mathcal{G}_2 , we also obtain an optimal transition coupling of the Markov chains P and Q . In particular, if (λ, R) is an optimal solution to Problem (3), then $\lambda(u, v)$ describes the alignment probability of vertices $u \in V_1$ and $v \in V_2$, while $\lambda(u, v)R((u, v), (u', v'))$ describes the alignment probability of the edges $(u, u') \in E_1$ and $(v, v') \in E_2$. Note that the optimal transition coupling also provides an alignment of higher-order paths, but we do not explore this observation any further here.

The GraphOTC problem brings the tools of Markov chain OT to bear on graphs. Moreover, GraphOTC incorporates both local information (by means of a cost) and global structure (via transition couplings). As we will demonstrate empirically in Sections 4 and 5, this results in an approach to graph OT that automatically balances vertex and edge information with topological structure in performing alignment and comparison.

GraphOTC is a metric. Building upon previous results in stationary optimal transport, one may establish that the GraphOTC cost is a metric on a certain space of graphs when the cost c is a metric. We will say that $\mathcal{G}_1 \sim \mathcal{G}_2$ for two graphs $\mathcal{G}_1 = (V, E, w_1)$ and $\mathcal{G}_2 = (V, E, w_2)$ if there exists $C \in \mathbb{R}$ such that $w_1(u, v) = w_2(u, v) + C$ for every $(u, v) \in E$. We prove in the Appendix A that $\mathcal{G}_1 \sim \mathcal{G}_2$ if and only if their respective random walks are identical.

Theorem 1. *Suppose that the cost function $c : V \times V \rightarrow \mathbb{R}_+$ satisfies the properties of a metric on V . Then d is a metric on the equivalence classes defined by \sim .*

The proof of Theorem 1 is deferred to Appendix A.

3.1 GraphOTC with intrinsic cost functions

The GraphOTC problem, along with several other graph OT methods, relies on the specification of a cost function $c : V_1 \times V_2 \rightarrow \mathbb{R}_+$. Commonly, the cost c may be derived from features associated with vertices in the graphs or from distances between vertices when both graphs are embedded in a common metric space. For example, if one has access to label functions $\ell_1 : V_1 \rightarrow \mathcal{A}$ and $\ell_2 : V_2 \rightarrow \mathcal{A}$ associating each vertex in V_1 and V_2 with a label in a finite alphabet \mathcal{A} , then one may let $c(u, v) = \delta(\ell_1(u) \neq \ell_2(v))$. We refer to this function as the 0-1 cost for the label functions ℓ_1 and ℓ_2 . Alternatively, if there exist maps $f_1 : V_1 \rightarrow \mathcal{U}$ and $f_2 : V_2 \rightarrow \mathcal{U}$ taking vertices in V_1 and V_2 to points in a metric space (\mathcal{U}, ρ) , then a cost may be defined as $c(u, v) = \rho(f_1(u), f_2(v))$ or $c(u, v) = \rho(f_1(u), f_2(v))^2$.

However, in some contexts such vertex features may be unavailable in practice, and one may wish to define a cost function when one is not given. In this case, one may consider costs defined in terms

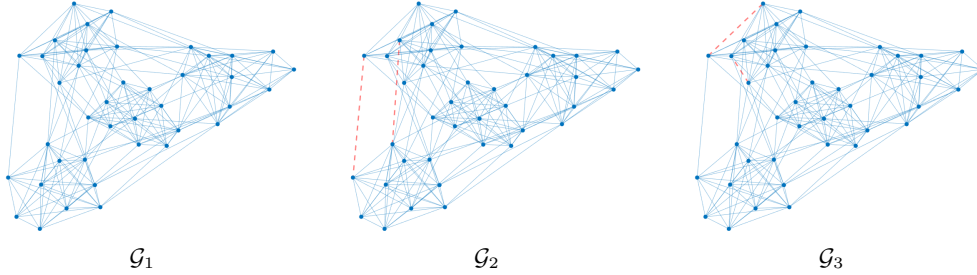


Figure 1: Three registered graphs with block structure. \mathcal{G}_1 was generated from a stochastic block model, \mathcal{G}_2 was obtained by removing two edges between blocks, and \mathcal{G}_3 was obtained by removing two edges within blocks. The removed edges of each graph are highlighted with red dashed lines.

of intrinsic properties of the graphs of interest. For example, letting $D_i : V_i \rightarrow \mathbb{N}$ be the degree function for graph \mathcal{G}_i , we might define the cost as $c_{\text{deg}}(u, v) = (D_1(u) - D_2(v))^2$. Alternatively, one may consider costs based on the degree distributions of the neighborhoods of u and v . Another approach is to embed the vertices in a Euclidean space *a priori* using graph embedding methods such as Laplacian eigenmaps [6]. We demonstrate in Section 4 that the squared-degree cost c_{deg} can adequately capture important graph structure when used with the GraphOTC problem.

3.2 Solving the GraphOTC problem

Given the graphs \mathcal{G}_1 and \mathcal{G}_2 , one may associate to each graph a stationary Markov chain, as described above. Once these Markov chains have been defined, solving the GraphOTC problem amounts to solving the OTC problem. Despite the non-convexity of the OTC problem, it was shown in [26] that one may obtain solutions via an adaptation of the policy iteration algorithm [16], referred to as ExactOTC. The algorithm ExactOTC exhibits a runtime scaling like $\mathcal{O}(|V_1||V_2|^3)$ per iteration. In practice, convergence is typically observed after less than 5 iterations. A more efficient algorithm based on entropic regularization and Sinkhorn iterations was proposed in [26] and is known as EntropicOTC. This algorithm was observed to scale better with the sizes of the marginal state spaces, yielding a runtime of $\mathcal{O}(|V_1||V_2|^2)$ per iteration (ignoring poly-logarithmic factors) in the case of GraphOTC. This runtime is nearly-linear in the dimension of couplings under consideration and in this sense is comparable to the state-of-the-art for entropic OT algorithms [28].

4 Examples

In this section, we compare GraphOTC to existing approaches for graph OT in a few examples.

4.1 Stochastic block models

Stochastic block models [15] (SBMs) are a common model for random graphs with group (or community) structure, and they have been used in a variety of applications, including community detection and graph clustering [1, 19, 2]. In an SBM, nodes are grouped into *blocks* representing communities within the graph. Edges are drawn between nodes independently at random with probabilities depending on whether the two nodes are within the same block or not. Generally, connection probabilities are higher within blocks than between blocks, leading to more densely connected subgraphs.

In order to develop some intuition about the behavior of various graph OT methods, we apply the GraphOTC distance along with existing graph OT methods to a selection of three graphs with block structure. The graphs of interest are depicted in Figure 1. \mathcal{G}_1 was drawn from an SBM with 40 nodes and 4 blocks, \mathcal{G}_2 was obtained by removing two edges between blocks from \mathcal{G}_1 , and \mathcal{G}_3 was

Table 1: Costs for graphs in Figure 1.

Algorithm	Chosen Cost	\mathcal{G}_1 vs. \mathcal{G}_2	\mathcal{G}_1 vs. \mathcal{G}_3	Ratio
GraphOTC	0-1	0.0396	0.0265	1.49
GraphOTC	c_{deg}	0.1718	0.1315	1.31
GW	–	0.1150	0.1125	1.02
GOT	–	0.0039	0.0019	2.05

obtained by removing two edges within blocks from \mathcal{G}_1 . Intuitively, the topology of a graph with block structure will depend more strongly on edges between blocks than within blocks and thus we regard \mathcal{G}_2 as more dissimilar to \mathcal{G}_1 than \mathcal{G}_3 is to \mathcal{G}_1 . In Table 1, we provide the distances computed by GraphOTC for two different costs, as well as distances computed by two other graph OT methods known as GW [24] and GOT [23], respectively. We find that GraphOTC and GOT regard \mathcal{G}_2 as more dissimilar from \mathcal{G}_1 than \mathcal{G}_3 is. On the other hand, GW detects little difference in the dissimilarity of the graphs. Similar results were observed for other choices of removed edges.

4.2 Wheel graphs

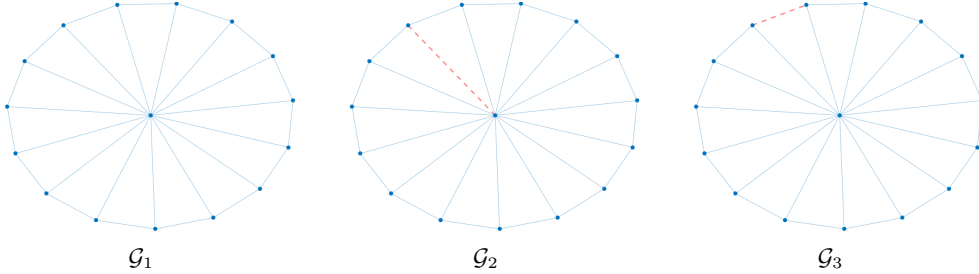


Figure 2: Three registered wheel graphs. \mathcal{G}_1 is a wheel graph of order 16, \mathcal{G}_2 was obtained by removing a spoke, and \mathcal{G}_3 was obtained by removing a wheel edge. The removed edges of each graph are highlighted with red dashed lines.

A wheel graph of order n is a graph containing a cycle of order $n - 1$ such that every node in the cycle is connected to a central node called a *hub*. The edges contained in the cycle are called wheel edges, and the edges connected to the hub are called *spoke edges* or *spokes* for short. We denote a wheel graph with n nodes by W_n .

Table 2: Costs for graphs in Figure 2.

Algorithm	Chosen Cost	\mathcal{G}_1 vs. \mathcal{G}_2	\mathcal{G}_1 vs. \mathcal{G}_3	Ratio
GraphOTC	0-1	0.0838	0.0607	1.38
GraphOTC	c_{deg}	2.6552	2.5517	1.04
GW	–	0.0512	0.0547	0.93
GOT	–	0.0459	0.0736	0.62

In Figure 2, we apply several different graph OT methods to two pairs of wheel-type graphs. The graph \mathcal{G}_1 is a wheel graph W_{16} , and \mathcal{G}_2 and \mathcal{G}_3 are both copies of \mathcal{G}_1 with one edge removed. \mathcal{G}_2 was obtained by removing a spoke and \mathcal{G}_3 was generated by removing a wheel edge from \mathcal{G}_1 . Since the hub node is connected with all other nodes, it is desirable for the topology of the wheel graph to depend more strongly on spokes than on wheel edges. Spokes contain the hub, while wheel edges do not. Thus, we expect \mathcal{G}_3 to be more similar to \mathcal{G}_1 than \mathcal{G}_2 is to \mathcal{G}_1 . In Table 2, we see GraphOTC detects that spokes are more influential than wheel edges, while GW and GOT do not. This provides some evidence that our approach accounts for differences in global structure when comparing graphs.

5 Experiments

In this section, we demonstrate the performance of GraphOTC on point cloud alignment and graph classification tasks. Complete experimental details may be found in Appendix C. In both experiments, we compare GraphOTC to the following graph OT baselines: standard optimal transport (OT), Gromov-Wasserstein (GW) [29], Fused Gromov-Wasserstein (FGW) [32, 33], and Coordinated Optimal Transport (COPT) [12]. We remark that GOT [24] solves an optimization problem which is nearly identical to COPT, so we omit it from our comparison. Code for reproducing the experiments may be found in the attached supplementary materials and will be released to the public upon publication. We note that this code makes use of the implementations of the ExactOTC and EntropicOTC algorithms provided at <https://github.com/oconnor-kevin/OTC>.

5.1 Point cloud alignment

In our first experiment, we consider the task of aligning graphs derived from point clouds. We consider randomly generated point clouds $D_1 = \{x_{1,1}, \dots, x_{1,N_1}\}$ and $D_2 = \{x_{2,1}, \dots, x_{2,N_2}\}$ in

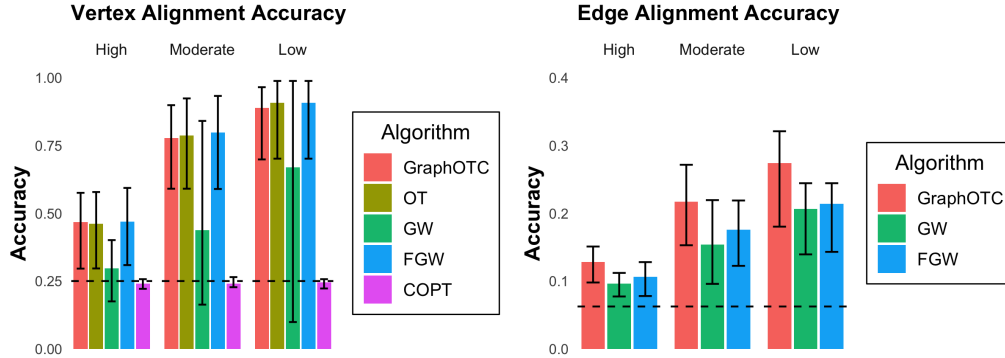


Figure 3: Point cloud alignment accuracies. We evaluate the alignment accuracies of each method in three different regimes: high overlap, moderate overlap, and low overlap (defined formally in Appendix C.1). Accuracies reported are the average observed over 5 random pairs of point clouds. The horizontal dashed line in each plot indicates the accuracy of random guessing.

\mathbb{R}^3 , independently drawn from a 4-component Gaussian mixture model as described in Appendix C.1. Given the point clouds D_1 and D_2 , the graph $\mathcal{G}_1 = (V_1, E_1, w_1)$ is defined to be the graph with vertex set $V_1 = D_1$, with edges and edge weights chosen as follows. Let $\lambda \geq 0$ and $\tilde{w}_1 \in \mathbb{R}^{|V_1| \times |V_1|}$ be the matrix such that for all $v_j, v_k \in V_1$, let $\tilde{w}_1(v_j, v_k) = -\lambda \|x_{1,j} - x_{1,k}\|_2$. In particular, λ allows one to tune the relative importance of the pairwise distances in determining the edge weights. If $\lambda = 0$, then all edges are given equal weight, while as λ becomes large, only edges between points that are very close to one another are given a non-negligible weight. Next, let w_1 be the edge weights obtained by rescaling the weights \tilde{w}_1 to lie in the interval $[0, 1]$ and then setting all weights that fall below 0.1 to 0. Finally, we remove all edges with weight equal to 0. The graph \mathcal{G}_2 corresponding to the other point cloud is constructed in the same way with the same λ .

In each iteration, we generate two graphs \mathcal{G}_1 and \mathcal{G}_2 as described above and apply each of the aforementioned graph OT methods to align the two graphs. Each method returns a soft alignment of the vertex sets V_1 and V_2 in the form of a coupling $\pi \in \Pi(p, q)$. Similarly, all methods other than COPT return an alignment of edges in the form of a 2-step coupling $\pi_{2\text{-step}} \in \mathcal{M}((V_1 \times V_2)^2)$. In the case of GW and FGW, $\pi_{2\text{-step}} = \pi \otimes \pi \in \Pi(p \otimes p, q \otimes q)$ while for GraphOTC, $\pi_{2\text{-step}} = \lambda \odot R \in \Pi(p \odot P, q \odot Q)$, for some (λ, R) in the OTC constraint set.

In Figure 3, we plot the vertex and edge alignment accuracies for each of the methods tested in the case $\lambda = 10^{-2}$. Similar results were observed for other values of λ in $\{10^{-5}, 10^{-4}, \dots, 10^{-1}\}$. Vertex alignment accuracy was assessed by summing the mass of the optimal coupling of the two graphs for pairs of vertices that were generated from the same mixture components. We find that OT, FGW, and GraphOTC perform roughly equivalently in the task of vertex alignment, while GW and COPT exhibit worse performance. In particular, COPT is only able to achieve an alignment accuracy roughly equivalent to random guessing. We suspect that this is because COPT is not able to take the geometric information into account in aligning the point cloud graphs.

We also compared the edge alignment accuracies of each algorithm in each of the three overlap regimes. Edge alignment accuracy was evaluated by summing the mass of the 2-step optimal coupling $\pi_{2\text{-step}}$ for pairs of edges connecting identical mixture components. We notice that GraphOTC outperforms FGW and GW from the standpoint of edge alignment. This provides further evidence that GraphOTC is able to balance local information (distances between nodes) with higher order structure in comparing the graphs of interest. Finally, we remark that the edge alignment accuracies were much lower than the vertex alignment accuracies observed for all algorithms. We suspect that this is due at least in part to the increased difficulty of edge alignment. In particular, random guessing for edge alignment yields an accuracy of 6.25% vs. 25% for vertex alignment.

5.2 Graph classification

In our next experiment, we demonstrate the utility of GraphOTC in a graph classification task. We consider a selection of benchmark graph datasets from [17] containing discrete vertex attributes as

well as a class label for every graph. This collection of datasets includes AIDS [30], BZR [31], Cuneiform [18], MCF-7 [37], MOLT-4 [37], MUTAG [10], and Yeast [37]. We obtain a cost function from the vertex attributes by letting the cost for a pair of vertices be equal to 0 if their labels are identical and 1 otherwise. Using this cost function, we fit a simple 5-nearest neighbor classifier using each of the graph OT costs to a randomly-sampled training set of graphs consisting of 80% of the data. In Table 3, we report the average classification accuracy observed on the held-out test set for each graph OT cost and dataset over 5 random samplings of the training and test sets.

Table 3: 5-nearest neighbor classification accuracies for graphs with discrete node attributes. Average accuracies observed over 5 random samplings of the training and test sets are reported along with their standard deviation.

Algorithm	AIDS	BZR	Cuneiform	MCF-7	MOLT-4	MUTAG	Yeast
GraphOTC	88.0 ± 4.9	84.8 ± 6.6	73.2 ± 7.8	92.8 ± 4.2	92.0 ± 2.0	85.4 ± 7.1	90.8 ± 6.4
OT	84.4 ± 6.1	76.4 ± 4.6	71.3 ± 7.7	93.6 ± 3.3	92.0 ± 2.0	63.2 ± 7.3	91.2 ± 7.0
GW	98.8 ± 1.8	78.0 ± 8.5	12.8 ± 4.6	93.6 ± 3.3	91.6 ± 2.6	81.6 ± 7.0	91.6 ± 6.2
FGW	99.2 ± 1.1	80.4 ± 7.4	71.7 ± 7.2	92.8 ± 4.2	91.2 ± 2.3	83.8 ± 8.3	90.0 ± 5.5
COPT	98.0 ± 1.4	73.6 ± 7.9	16.6 ± 3.1	92.4 ± 4.8	91.6 ± 2.6	80.0 ± 5.6	90.4 ± 6.7

In Table 3, we see that GraphOTC outperforms the baseline methods in several cases. We emphasize that GraphOTC is competitive with other graph OT methods without the need for tuning any hyperparameters. This suggests that GraphOTC sufficiently captures important differences among the graphs of interest by default and provides further support for the proposed approach. When taking standard deviations into account, we do not see significant differences in performance between the algorithms in most cases. Therefore, it would be helpful to perform a more detailed study in the future with a greater number of training-test set randomizations.

6 FusedOTC

In this section, we describe a more general framework of graph OT problems that includes both GraphOTC and OT of the stationary distributions as extremal cases. This more general framework is analogous to the Fused Gromov-Wasserstein distance proposed in [32]. Specifically, in order to more flexibly capture global and local differences in the graphs of interest, we augment the GraphOTC objective, adding a term that penalizes changes in edge weights (as in GW). We refer to the resulting graph OT problem as FusedOTC. We show in Theorem 2 that one may recover both the GraphOTC and standard OT costs as special cases of FusedOTC by taking appropriate limits.

Let $\alpha \in [0, 1]$ and let $p \in \Delta_{|V_1|}$ and $q \in \Delta_{|V_2|}$ be the stationary distributions of the chains P and Q . The Fused Gromov-Wasserstein (FGW) problem [32] for graphs $\mathcal{G}_1 = (V_1, E_1, w_1)$ and $\mathcal{G}_2 = (V_2, E_2, w_2)$ may be written in a simplified form as

$$d_{\alpha}^{\text{FGW}}(\mathcal{G}_1, \mathcal{G}_2) = \min \{ \alpha \langle \pi, c \rangle + (1 - \alpha) \langle \pi \otimes \pi, E \rangle : \pi \in \Pi(p, q) \}, \quad (4)$$

where $E \in \mathbb{R}^{|V_1| \times |V_2| \times |V_1| \times |V_2|}$ is the matrix satisfying $E((u, v), (u', v')) = |w_1(u, u') - w_2(v, v')|$. Note that compared to the standard OT distance between p and q , the objective in Problem (4) includes an additional term penalizing changes in edge weights. Depending on one's choice of α , the FGW problem will prioritize coupling similar vertices or similar edge weights. In the case that $\alpha = 1$, one recovers the standard OT problem for marginals p and q and cost c , while in the case that $\alpha = 0$, one recovers the Gromov-Wasserstein problem for graphs \mathcal{G}_1 and \mathcal{G}_2 .

We may extend the flexibility of the FGW problem to GraphOTC in a straightforward manner, yielding a graph OT problem that can adaptively balance expected cost with correct edge coupling while taking global graph structure into account. We refer to this problem as the FusedOTC problem. Fixing parameters $\alpha \in [0, 1]$ and $\tau \in \mathbb{N}$, the FusedOTC problem is defined as

$$d_{\tau, \alpha}(\mathcal{G}_1, \mathcal{G}_2) = \min \{ \alpha \langle \lambda, c \rangle + (1 - \alpha) \langle \lambda \odot R, E \rangle : R \in \Pi_{\text{TC}}(P^{\tau}, Q^{\tau}), \lambda R = \lambda, \lambda \in \Delta_{|V_1| \times |V_2|} \}.$$

The FusedOTC problem is highly flexible and generalizes both the GraphOTC problem as well as the standard OT problem between the stationary distributions of the chains P and Q . In the case $\alpha = 1$ and $\tau = 1$, we recover the GraphOTC problem, while in the case $\alpha = 0$ and $\tau \in \mathbb{N}$, we obtain a

new graph OT problem that is independent of the cost c . Relying on basic results in Markov chain theory, we expect that in the limit $\tau \rightarrow \infty$, the chains P^τ and Q^τ become IID. In this limit and with $\alpha = 1$, we recover the Wasserstein distance (d^W) between the stationary distributions $p \in \Delta_{|V_1|}$ and $q \in \Delta_{|V_2|}$ of the Markov chains P and Q . These properties are formalized in the following theorem, whose proof appears in Appendix B.

Theorem 2. *The FusedOTC cost $d_{\tau,\alpha}$ satisfies the following:*

$$\bullet \lim_{\alpha \rightarrow 1} d_{1,\alpha}(\mathcal{G}_1, \mathcal{G}_2) = d(\mathcal{G}_1, \mathcal{G}_2) \qquad \bullet \lim_{(\tau,\alpha) \rightarrow (\infty,1)} d_{\tau,\alpha}(\mathcal{G}_1, \mathcal{G}_2) = d^W(\mathcal{G}_1, \mathcal{G}_2)$$

7 Discussion

In this paper, we proposed the GraphOTC problem for comparing and aligning graphs. This new approach to graph OT applies ideas from constrained OT for Markov chains to the random walks associated to the graphs. In theory and practice, we demonstrated that GraphOTC balances differences in both global and local structure. In synthetic and real data experiments, we showed that GraphOTC exhibits equal or better performance to state-of-the-art graph OT methods in both comparison and alignment tasks. We also described a more flexible framework for graph OT known as FusedOTC, from which one may recover both GraphOTC as well as standard OT as special cases. Future work may aim to develop computationally tractable algorithms for solving the FusedOTC problem and explore principled means of selecting the hyperparameters α and τ in practice.

Graph-structured data may be found in a wide variety of application areas. The GraphOTC problem offers a novel approach to studying this data from the perspective of Markov chains and optimal transport. We showed that GraphOTC achieves the state-of-the-art in graph OT for a 5-nearest neighbor classification task for several real datasets including BZR, MOLT-4, and MUTAG. Graphs in each of these datasets describe molecular structure for different compounds of interest. Consequently, GraphOTC may find application in this area, enabling practitioners to compare and align molecules. Potential applications beyond biochemistry might include the analysis of social networks or protein-protein interaction networks. While GraphOTC does not present any direct opportunities for negative societal impacts, indirect negative effects are possible in each of the potential applications mentioned.

This study has several limitations. While GraphOTC performs well in the experiments presented here, other methods may be better suited to particular tasks. Additionally, further experiments are necessary to characterize the performance of GraphOTC fully. Lastly, we note that all of the currently available graph OT methods, including GraphOTC, may present computational challenges for large graphs.

Acknowledgments and Disclosure of Funding

KO and ABN were supported in part by NSF grants DMS-1613072 and DMS-1613261. KM gratefully acknowledges the support of NSF CAREER grant DMS-1847144.

References

- [1] E. Abbe. Community detection and stochastic block models: Recent developments. *Journal of Machine Learning Research*, 18(177):1–86, 2018.
- [2] E. Abbe and C. Sandon. Community detection in general stochastic block models: Fundamental limits and efficient algorithms for recovery. *2015 IEEE 56th Annual Symposium on Foundations of Computer Science*, pages 670–688, 2015.
- [3] D. Aldous and J. Fill. Reversible Markov chains and random walks on graphs, 2002.
- [4] D. Alvarez-Melis and T. Jaakkola. Gromov-Wasserstein alignment of word embedding spaces. In *Proceedings of the 2018 Conference on Empirical Methods in Natural Language Processing*, pages 1881–1890, 2018.
- [5] A. Barbe, M. Sebban, P. Gonçalves, P. Borgnat, and R. Gribonval. Graph diffusion Wasserstein distances. In *European Conference on Machine Learning and Principles and Practice of Knowledge Discovery in Databases*, 2020.

- [6] M. Belkin and P. Niyogi. Laplacian eigenmaps for dimensionality reduction and data representation. *Neural computation*, 15(6):1373–1396, 2003.
- [7] J. F. Bonnans and A. Shapiro. *Perturbation analysis of optimization problems*. Springer Science & Business Media, 2013.
- [8] L. Chen, Z. Gan, Y. Cheng, L. Li, L. Carin, and J. Liu. Graph optimal transport for cross-domain alignment. In *International Conference on Machine Learning*, pages 1542–1553. PMLR, 2020.
- [9] T. de la Rue. Joinings in ergodic theory. In *Mathematics of Complexity and Dynamical Systems*.
- [10] A. K. Debnath, R. L. Lopez de Compadre, G. Debnath, A. J. Shusterman, and C. Hansch. Structure-activity relationship of mutagenic aromatic and heteroaromatic nitro compounds. correlation with molecular orbital energies and hydrophobicity. *Journal of medicinal chemistry*, 34(2):786–797, 1991.
- [11] P. Demetci, R. Santorella, B. Sandstede, W. S. Noble, and R. Singh. Gromov-Wasserstein optimal transport to align single-cell multi-omics data. *BioRxiv*, 2020.
- [12] Y. Dong and W. Sawin. Copt: Coordinated optimal transport on graphs. *Advances in Neural Information Processing Systems*, 33, 2020.
- [13] H. Furstenberg. Disjointness in ergodic theory, minimal sets, and a problem in diophantine approximation. *Theory of Computing Systems*, 1(1):1–49, 1967.
- [14] R. M. Gray, D. L. Neuhoff, and P. C. Shields. A generalization of Ornstein’s \bar{d} distance with applications to information theory. *The Annals of Probability*, pages 315–328, 1975.
- [15] P. W. Holland, K. B. Laskey, and S. Leinhardt. Stochastic blockmodels: First steps. *Social Networks*, 5:109–137, 1983.
- [16] R. A. Howard. Dynamic programming and Markov processes. 1960.
- [17] K. Kersting, N. M. Kriege, C. Morris, P. Mutzel, and M. Neumann. Benchmark data sets for graph kernels, 2016. <http://graphkernels.cs.tu-dortmund.de>.
- [18] N. M. Kriege, M. Fey, D. Fisseler, P. Mutzel, and F. Weichert. Recognizing cuneiform signs using graph based methods. In *International Workshop on Cost-Sensitive Learning*, pages 31–44. PMLR, 2018.
- [19] C. Lee and D. Wilkinson. A review of stochastic block models and extensions for graph clustering. *Applied Network Science*, 4:1–50, 2019.
- [20] D. A. Levin and Y. Peres. *Markov chains and mixing times*, volume 107. American Mathematical Soc., 2017.
- [21] L. Lovász et al. Random walks on graphs: A survey. *Combinatorics, Paul erdos is eighty*, 2(1):1–46, 1993.
- [22] J. Malka, R. Flamary, and N. Courty. Gromov-Wasserstein optimal transport for heterogeneous domain adaptation.
- [23] H. P. Maretic, M. E. Gheche, G. Chierchia, and P. Frossard. Got: An optimal transport framework for graph comparison. *Advances in Neural Information Processing Systems 32*, 32(CONF), 2019.
- [24] H. P. Maretic, M. E. Gheche, M. Minder, G. Chierchia, and P. Frossard. Wasserstein-based graph alignment. *arXiv preprint arXiv:2003.06048*, 2020.
- [25] F. Mémoli. Gromov–Wasserstein distances and the metric approach to object matching. *Foundations of computational mathematics*, 11(4):417–487, 2011.
- [26] K. O’Connor, K. McGoff, and A. Nobel. Optimal transport for stationary Markov chains via policy iteration. *arXiv preprint arXiv:2006.07998*, 2020.
- [27] D. S. Ornstein. An application of ergodic theory to probability theory. *The Annals of Probability*, 1(1):43–58, 1973.
- [28] G. Peyré, M. Cuturi, et al. Computational optimal transport. *Foundations and Trends® in Machine Learning*, 11(5-6):355–607, 2019.
- [29] G. Peyré, M. Cuturi, and J. Solomon. Gromov-Wasserstein averaging of kernel and distance matrices. In *International Conference on Machine Learning*, pages 2664–2672. PMLR, 2016.

- [30] K. Riesen and H. Bunke. Iam graph database repository for graph based pattern recognition and machine learning. In *Joint IAPR International Workshops on Statistical Techniques in Pattern Recognition (SPR) and Structural and Syntactic Pattern Recognition (SSPR)*, pages 287–297. Springer, 2008.
- [31] J. J. Sutherland, L. A. O’Brien, and D. F. Weaver. Spline-fitting with a genetic algorithm: A method for developing classification structure- activity relationships. *Journal of chemical information and computer sciences*, 43(6):1906–1915, 2003.
- [32] V. Titouan, N. Courty, R. Tavenard, and R. Flamary. Optimal transport for structured data with application on graphs. In *International Conference on Machine Learning*, pages 6275–6284, 2019.
- [33] T. Vayer, L. Chapel, R. Flamary, R. Tavenard, and N. Courty. Fused Gromov-Wasserstein distance for structured objects. *Algorithms*, 13(9):212, 2020.
- [34] T. Vayer, R. Flamary, R. Tavenard, L. Chapel, and N. Courty. Sliced Gromov-Wasserstein. In *NeurIPS 2019-Thirty-third Conference on Neural Information Processing Systems*, volume 32, 2019.
- [35] H. Xu, D. Luo, and L. Carin. Scalable Gromov-Wasserstein learning for graph partitioning and matching. In *Advances in Neural Information Processing Systems*, pages 3052–3062, 2019.
- [36] H. Xu, D. Luo, H. Zha, and L. C. Duke. Gromov-Wasserstein learning for graph matching and node embedding. In *International Conference on Machine Learning*, pages 6932–6941. PMLR, 2019.
- [37] X. Yan. <https://sites.cs.ucsb.edu/~xyan/dataset.htm>.
- [38] Y. Yan, W. Li, H. Wu, H. Min, M. Tan, and Q. Wu. Semi-supervised optimal transport for heterogeneous domain adaptation. In *IJCAI*, volume 7, pages 2969–2975, 2018.

A Proof of Theorem 1

In this appendix, we prove Theorem 1, concluding that the GraphOTC cost is a metric on a certain set of equivalence classes of graphs. We begin by proving the following lemma, which states that two graphs are equivalent if and only if they have identical associated transition matrices.

Lemma A.1. *For two graphs $\mathcal{G}_1 = (V, E, w_1)$ and $\mathcal{G}_2 = (V, E, w_2)$ with associated Markov transition matrices P and Q , $\mathcal{G}_1 \sim \mathcal{G}_2$ if and only if P and Q are equal.*

Proof. Suppose first that $\mathcal{G}_1 \sim \mathcal{G}_2$ and thus there exists C such that $w_1(u, v) = w_2(u, v) + C$ for every $(u, v) \in E$. Then clearly the two transition matrices P and Q associated with \mathcal{G}_1 and \mathcal{G}_2 are equal. Now suppose that P and Q are equal. Then for every $(u, v) \in E$, we have

$$\frac{\exp\{w_1(u, v)\}}{\sum_{\tilde{v}:(u, \tilde{v}) \in E} \exp\{w_1(u, \tilde{v})\}} = \frac{\exp\{w_2(u, v)\}}{\sum_{\tilde{v}:(u, \tilde{v}) \in E} \exp\{w_2(u, \tilde{v})\}}.$$

Written another way, we have $w_1(u, v) = w_2(u, v) + C_u$, where

$$C_u = \ln \left(\frac{\sum_{\tilde{v}:(u, \tilde{v}) \in E} \exp\{w_1(u, \tilde{v})\}}{\sum_{\tilde{v}:(u, \tilde{v}) \in E} \exp\{w_2(u, \tilde{v})\}} \right).$$

Since \mathcal{G}_1 and \mathcal{G}_2 are undirected, $(v, u) \in E$ and a similar argument will establish that $w_1(v, u) = w_2(v, u) + C_v$. The undirectedness of \mathcal{G}_1 and \mathcal{G}_2 also implies that $w_1(u, v) = w_1(v, u)$ and $w_2(u, v) = w_2(v, u)$. It follows that $w_1(v, u) = w_2(v, u) + C_u$ and thus $C_u = C_v$. Since \mathcal{G}_1 and \mathcal{G}_2 are connected, there exists a sequence of edges $(u_1, u_2), (u_2, u_3), \dots, (u_{n-1}, u_n) \in E$ such that $u \in \{u_1, \dots, u_n\}$ for every $u \in V$. Iterating the arguments above for all edges in this sequence we conclude that $C_u = C_v$ for every $u, v \in V$. It follows that $w_1(u, v) = w_2(u, v) + C$ for some constant C that is independent of u and v . Then by definition, $\mathcal{G}_1 \sim \mathcal{G}_2$ and the claim is proven. \square

Before proceeding with the proof of Theorem 1, we introduce some necessary background. We will make use of the optimal joining distance $\bar{\rho}$ [27, 14] between stationary processes. Informally, for stationary processes X and Y taking values in finite sets \mathcal{X} and \mathcal{Y} , the optimal joining distance $\bar{\rho}(X, Y)$ with respect to $c : \mathcal{X} \times \mathcal{Y} \rightarrow \mathbb{R}$ is obtained by minimizing $\mathbb{E}[c(\tilde{X}, \tilde{Y})]$ over the set of jointly stationary paired processes (\tilde{X}, \tilde{Y}) taking values in $\mathcal{X} \times \mathcal{Y}$ such that \tilde{X} and \tilde{Y} are equal in distribution to X and Y , respectively. Such processes are referred to as *joinings* of X and Y [13, 9]. Since every transition coupling of stationary Markov chains P and Q is also a joining of P and Q , we have

$$\bar{\rho}(P, Q) \leq \min \{ \langle \lambda, c \rangle : R \in \Pi_{\text{TC}}(P, Q), \lambda R = \lambda, \lambda \in \Delta_{|\mathcal{X}| \times |\mathcal{Y}|} \}.$$

In particular, if the chains P and Q are associated with graphs $\mathcal{G}_1 = (\mathcal{X}, E_1, w_1)$ and $\mathcal{G}_2 = (\mathcal{Y}, E_2, w_2)$, $\bar{\rho}(P, Q) \leq d(\mathcal{G}_1, \mathcal{G}_2)$. Finally, we remark that in the case that $\mathcal{X} = \mathcal{Y}$, $\bar{\rho}(\cdot, \cdot)$ is known to satisfy the properties of a metric when c does [14].

Theorem 1. *Suppose that the cost function $c : V \times V \rightarrow \mathbb{R}_+$ satisfies the properties of a metric on V . Then d is a metric on the equivalence classes defined by \sim .*

Proof. The symmetry of d is clear. Moreover, it was established in [26] that the optimal transition coupling cost satisfies the triangle inequality for Markov chains when the cost c does. Thus d satisfies the triangle inequality for graphs. So it suffices to show that $d(\mathcal{G}_1, \mathcal{G}_2) = 0$ if and only if $\mathcal{G}_1 \sim \mathcal{G}_2$. Let \mathcal{G}_1 and \mathcal{G}_2 be graphs satisfying $\mathcal{G}_1 \sim \mathcal{G}_2$ with associated transition matrices P and Q . By Lemma A.1, P and Q are equal and clearly $d(\mathcal{G}_1, \mathcal{G}_2) = 0$ since $\langle \lambda, c \rangle = 0$ is achieved by λ satisfying $\lambda(u, v) = p(u)\delta(u = v)$, which is stationary for the transition coupling satisfying $R((u, v), (u', v')) = P(u, u')\delta(u = v)\delta(u' = v')$. Now suppose that $\mathcal{G}_1 \not\sim \mathcal{G}_2$. Again by Lemma A.1, the transition matrices P and Q are distinct and consequently so are their associated stationary Markov chains. Since it defines a distance on stationary processes, the optimal joining distance satisfies $\bar{\rho}(P, Q) > 0$. Since the optimal transition coupling cost is lower bounded by the optimal joining distance $\bar{\rho}(\cdot, \cdot)$, it follows that

$$0 < \bar{\rho}(P, Q) \leq \min \{ \langle \lambda, c \rangle : R \in \Pi_{\text{TC}}(P, Q), \lambda R = \lambda, \lambda \in \Delta_{|V| \times |V|} \} = d(\mathcal{G}_1, \mathcal{G}_2).$$

Thus $d(\mathcal{G}_1, \mathcal{G}_2) = 0$ if and only if $\mathcal{G}_1 \sim \mathcal{G}_2$ and the proof is concluded. \square

B Proof of Theorem 2

Our proof of Theorem 2 follows an argument similar to the proof of [26, Theorem 11], which establishes a stability result for the OTC problem. Our proof utilizes a well-known stability result, detailed in Lemma B.1 below, for optimization problems satisfying certain conditions. Before stating this result, we fix some notation and definitions. Let \mathcal{Z} and \mathcal{U} be Polish spaces corresponding to a set of possible solutions and a set of parameters, respectively. Then for a function $f : \mathcal{Z} \times \mathcal{U} \rightarrow \mathbb{R}$ and feasible set $\Phi : \mathcal{U} \rightarrow 2^{\mathcal{Z}}$, consider the optimization problem indexed by a parameter $u \in \mathcal{U}$,

$$\min\{f(z, u) : z \in \Phi(u)\}. \quad (5)$$

Note that $f(\cdot, u) : \mathcal{Z} \rightarrow \mathbb{R}$ describes the objective to be minimized and $\Phi(u) \subset \mathcal{Z}$ represents the feasible set of Problem (5). We will call a set $\mathcal{V} \subset \mathcal{Z}$ a neighborhood of a subset $\mathcal{W} \subset \mathcal{Z}$ if $\mathcal{W} \subset \text{int } \mathcal{V}$. Neighborhoods in \mathcal{U} will be defined similarly. Now we may state the key lemma for the proof of Theorem 2.

Lemma B.1 ([7], Proposition 4.4). *Let u_0 be a given point in the parameter space \mathcal{U} . Suppose that (i) the function $f(z, u)$ is continuous on $\mathcal{Z} \times \mathcal{U}$, (ii) the graph of the multifunction $\Phi(\cdot)$ is a closed subset of $\mathcal{U} \times \mathcal{Z}$, (iii) there exists $a \in \mathbb{R}$ and a compact set $C \subset \mathcal{Z}$ such that for every u in a neighborhood of u_0 , the level set $\{z \in \Phi(u) : f(z, u) \leq a\}$ is nonempty and contained in C , (iv) for any neighborhood $\mathcal{V}_{\mathcal{Z}}$ of the set $\text{argmin}_{z \in \Phi(u_0)} f(z, u_0)$ there exists a neighborhood $\mathcal{V}_{\mathcal{U}}$ of u_0 such that $\mathcal{V}_{\mathcal{Z}} \cap \Phi(u) \neq \emptyset$ for all $u \in \mathcal{V}_{\mathcal{U}}$. Then the optimal value function $u \mapsto \min_{z \in \Phi(u)} f(z, u)$ is continuous at $u = u_0$.*

In order to simplify notation going forward, we will assume without loss of generality that the vertex sets V_1 and V_2 satisfy $|V_1| = |V_2| = d$ for some $d \in \mathbb{N}$. Moreover, we will make use of the fact that the set of $d \times d$ (resp. $d^2 \times d^2$) transition matrices may be identified with the set Δ_d^d (resp. $\Delta_{d^2}^{d^2}$). Now, let

$$\mathcal{Z} = \left\{ (\lambda, R) \in \Delta_{d^2} \times \Delta_{d^2}^{d^2} : R \in \Pi_{\text{TC}}(P, Q) \text{ for some } P, Q \in \Delta_d^d, \lambda R = \lambda \right\}$$

be the union of all feasible sets for the FusedOTC problem and $\mathcal{U} = \text{cl}\{(P^\tau, Q^\tau) : \tau \in \mathbb{N}\} \times [0, 1]$ be the set of all valid pairs (P^τ, Q^τ, α) including the limit $(\bar{P}, \bar{Q}, \alpha)$ where $\bar{P} = \lim_{\tau \rightarrow \infty} P^\tau$ and $\bar{Q} = \lim_{\tau \rightarrow \infty} Q^\tau$. Note that since P and Q are aperiodic and irreducible, \bar{P} and \bar{Q} exist and have rows equal to the stationary distributions p and $q \in \Delta_d$ of P and Q , respectively. One may easily verify that \mathcal{Z} and \mathcal{U} are compact subsets of $\mathbb{R}^{d^2} \times \mathbb{R}^{d^2 \times d^2}$ and $\mathbb{R}^{d \times d} \times \mathbb{R}^{d \times d} \times \mathbb{R}$, respectively. The objective function $f(\cdot, \cdot)$ is identified with the map

$$((\lambda, R), (P^\tau, Q^\tau, \alpha)) \mapsto \alpha \langle c, \lambda \rangle + (1 - \alpha) \langle E, \lambda \odot R \rangle,$$

which does not depend on P^τ or Q^τ . We will refer to the constraint functions for the FusedOTC problem by $\Phi : \mathcal{U} \rightarrow 2^{\mathcal{Z}}$. In particular, we let

$$\Phi((P^\tau, Q^\tau, \alpha)) = \left\{ (\lambda, R) \in \Delta_{d^2} \times \Delta_{d^2}^{d^2} : R \in \Pi_{\text{TC}}(P^\tau, Q^\tau), \lambda R = \lambda, \lambda \in \Delta_{d^2} \right\}.$$

Now we may proceed with the proof of Theorem 2.

Theorem 2. *The FusedOTC cost $d_{\tau, \alpha}$ satisfies the following:*

$$\bullet \lim_{\alpha \rightarrow 1} d_{1, \alpha}(\mathcal{G}_1, \mathcal{G}_2) = d(\mathcal{G}_1, \mathcal{G}_2) \quad \bullet \lim_{(\tau, \alpha) \rightarrow (\infty, 1)} d_{\tau, \alpha}(\mathcal{G}_1, \mathcal{G}_2) = d^w(\mathcal{G}_1, \mathcal{G}_2)$$

Proof. We begin by proving the second claim. It will suffice to check the conditions of Lemma B.1 for the FusedOTC problem at the point $u_0 = (\bar{P}, \bar{Q}, 1) \in \mathcal{U}$. First, (i) clearly holds since the objective $f(\cdot, \cdot)$ is quadratic in (λ, R) , linear in α , and does not depend on P^τ or Q^τ . Next, we will show that the graph of $\Phi(\cdot)$ is a closed subset of $\mathcal{U} \times \mathcal{Z}$. Fix a sequence $\{(P_n, Q_n, \alpha_n, \lambda_n, R_n)\}_{n \geq 1} \subset \text{graph } \Phi(\cdot)$. As a subset of the compact set $\Delta_d^d \times \Delta_d^d \times [0, 1] \times \Delta_{d^2} \times \Delta_{d^2}^{d^2}$, it has a subsequence, which we also label as $\{(P_n, Q_n, \alpha_n, \lambda_n, R_n)\}_{n \geq 1}$ converging to some $(P', Q', \alpha', \lambda', R') \in \Delta_d^d \times \Delta_d^d \times [0, 1] \times \Delta_{d^2} \times \Delta_{d^2}^{d^2}$. Taking limits of the linear equations $R_n \in \Pi_{\text{TC}}(P_n, Q_n)$ and $\lambda_n R_n = \lambda_n$, we conclude that $R' \in \Pi_{\text{TC}}(P', Q')$ and $\lambda' R' = \lambda'$. Thus $(P', Q', \alpha', \lambda', R') \in \text{graph } \Phi(\cdot)$ and (ii) holds. To show that (iii) is satisfied, note that one may let $a = \|c\|_\infty + \|E\|_\infty$ and use the fact that the entire

set \mathcal{Z} is compact. Finally, we will show that (iv) is satisfied. Let $\mathcal{V}_{\mathcal{Z}} \subset \mathcal{Z}$ be a neighborhood of $\operatorname{argmin}_{z \in \Phi(u_0)} f(z, u_0)$. Then define the neighborhood $\mathcal{V}_{\mathcal{U}}$ of $u_0 = (\bar{P}, \bar{Q}, 1)$ as

$$\mathcal{V}_{\mathcal{U}} := \{(P, Q) \in \Delta_d^d \times \Delta_d^d : R \in \Pi_{\text{TC}}(P, Q) \text{ for some } (\lambda, R) \in \mathcal{V}_{\mathcal{Z}} \times \{1\}\}.$$

Note that $\mathcal{V}_{\mathcal{U}}$ is nonempty by the non-emptiness of $\mathcal{V}_{\mathcal{Z}}$ and the definition of \mathcal{Z} . Moreover, $\mathcal{V}_{\mathcal{Z}} \cap \Phi(u) \neq \emptyset$ for all $u \in \mathcal{V}_{\mathcal{U}}$ by construction. Thus all the conditions of Lemma B.1 are satisfied and we conclude that $u \mapsto \min_{z \in \Phi(u)} f(z, u)$ is continuous at $u_0 = (\bar{P}, \bar{Q}, 1)$. Letting $u(\tau, \alpha) = (P^\tau, Q^\tau, \alpha)$, the continuity of $u(\cdot, \cdot)$ implies that the map $(\tau, \alpha) \mapsto \min_{z \in \Phi(u(\tau, \alpha))} f(z, u(\tau, \alpha))$ satisfies

$$\lim_{(\tau, \alpha) \rightarrow (\infty, 1)} d_{\tau, \alpha}(\mathcal{G}_1, \mathcal{G}_2) = \lim_{(\tau, \alpha) \rightarrow (\infty, 1)} \min_{z \in \Phi(u(\tau, \alpha))} f(z, u(\tau, \alpha)) = \min_{z \in \Phi(\bar{P}, \bar{Q}, 1)} f(z, (\bar{P}, \bar{Q}, 1)).$$

In particular,

$$\lim_{(\tau, \alpha) \rightarrow (\infty, 1)} d_{\tau, \alpha}(\mathcal{G}_1, \mathcal{G}_2) = \min \{ \langle \lambda, c \rangle : R \in \Pi_{\text{TC}}(\bar{P}, \bar{Q}), \lambda R = \lambda, \lambda \in \Delta_{|V_1| \times |V_2|} \}.$$

Since the chains associated with \bar{P} and \bar{Q} are IID, the OTC cost between them is simply the standard OT cost between their respective stationary distributions p and q . As a consequence, we find that

$$\lim_{(\tau, \alpha) \rightarrow (\infty, 1)} d_{\tau, \alpha}(\mathcal{G}_1, \mathcal{G}_2) = d^{\text{W}}(\mathcal{G}_1, \mathcal{G}_2).$$

Using the same line of reasoning as above, one may establish that the map $u \mapsto \min_{z \in \Phi(u)} f(z, u)$ is continuous at $u_0 = (P, Q, \alpha)$ for any $\alpha \in [0, 1]$. Letting $u(\alpha) = (P, Q, \alpha)$, the continuity of the $u(\cdot)$ implies that $\alpha \mapsto \min_{z \in \Phi(u(\alpha))} f(z, u(\alpha))$ is continuous at 1 and thus

$$\lim_{\alpha \rightarrow 1} d_{1, \alpha}(\mathcal{G}_1, \mathcal{G}_2) = \lim_{\alpha \rightarrow 1} \min_{z \in \Phi(u(\alpha))} f(z, u(\alpha)) = \min_{z \in \Phi(u(1))} f(z, u(1)) = d(\mathcal{G}_1, \mathcal{G}_2).$$

This concludes the proof. \square

C Experimental details

In this appendix, we provide further details for the experiments discussed in Section 5.

C.1 Point cloud alignment

In the experiment described in Section 5.1, point clouds in \mathbb{R}^3 were generated from a 4-component Gaussian mixture model as follows: For a given $\sigma_\mu > 0$, we generate $\mu_1, \dots, \mu_4 \sim \mathcal{N}_3(0, \sigma_\mu^2 \mathbf{I})$ independently. The vectors μ_1, \dots, μ_4 will be the means of the four mixture components under consideration. Note that as σ_μ is increased, these means will tend to be further separated and the task of distinguishing between points from each component becomes easier. Then given $n_i \in \mathbb{N}$, we generate n_i points IID from $\mathcal{N}_3(\mu_i, \mathbf{I})$ for each $i = 1, \dots, 4$. Gathering these points, we obtain a point cloud $D \subset \mathbb{R}^3$ of size $N := \sum_{i=1}^4 n_i$.

The overlap regimes referred to in Figure 3 of Section 5.1 correspond to $\sigma_\mu = 1$ (high overlap), $\sigma_\mu = 2$ (moderate overlap), and $\sigma_\mu = 3$ (low overlap). In each iteration, we sampled 10 points from each mixture component to form the first graph and 5 points from each mixture component to form the second graph. For each choice of σ_μ , cross validation was performed for FGW (to select $\alpha \in \{0, 0.1, \dots, 1\}$) by randomly generating 5 pairs of graphs and computing alignments of vertices and edges. Parameters that yielded the highest average alignment accuracy were selected. Separate parameters were chosen for optimizing vertex and edge alignment. The `ExactOTC` algorithm [26] was used to compute solutions to the GraphOTC problem. The experiment was developed and run in Matlab on a 6-core, personal machine.

C.2 Graph classification

In order to compute approximate solutions to the GraphOTC problem, we used the `EntropicOTC` algorithm [26] with $L = 10$, $T = 50$, $\xi = 100$, and 50 Sinkhorn iterations. The FGW cost was computed with a default parameter choice of $\alpha = 0.5$. The experiment was developed in Matlab and run on a 24-core node in a university-owned computing cluster.